

# 13-kV Rectifiers: Studies on Diodes and Asymmetric Thyristors

F.-J. Niedernostheide<sup>a)</sup>, H.-J. Schulze<sup>a)</sup>, U. Kellner-Werdehausen<sup>b)</sup>,  
R. Barthelmess<sup>b)</sup>, J. Przybilla<sup>b)</sup>, R. Keller<sup>b)</sup>, H. Schoof<sup>b)</sup>, D. Pikorz<sup>b)</sup>

a) Infineon AG, Balanstr. 59, D-81541 Munich, Germany,  
e-mail: [franz-josef.niedernostheide@infineon.com](mailto:franz-josef.niedernostheide@infineon.com)

b) eupec GmbH, Max-Planck-Str. 5, D-59581 Warstein, Germany

**Abstract.** For rectifiers with high blocking voltages, the application of field stop layers reduces power losses. Preliminary experimental results are presented from asymmetric 13-kV thyristor samples based on a conventional field stop concept. By connecting a 13-kV diode in series to this asymmetric thyristor, a symmetrically-blocking tandem device can be built. Numerical studies show that the turn-off behavior of the 13-kV diode required for the tandem solution can be significantly improved by a new field stop concept based on an  $n$  layer buried in the weakly-doped region of the  $p^+ - n - n^+$  power diode.

## INTRODUCTION

The main objectives of development in high-power thyristor converters are the reduction of fabrication costs and greater reliability [1]. A promising way to achieve this is to increase the blocking voltage of the thyristors so that the number of thyristors connected in series can be reduced. For high blocking voltages, a series connection of an asymmetric thyristor and a diode has lower power losses than a symmetrically blocking thyristor. Furthermore, both devices can be utilized separately in specific high-voltage applications [2,3]. For example, asymmetric light-triggered thyristors can be favorably used in pulse-power applications where energy storage capacitors or inductors have to be discharged. High-voltage diodes are very valuable in crow bar applications to protect capacitors against charging with the reversed polarity.

In the first part of this paper, we describe some specifics of the 13-kV thyristor design, and present initial experimental results. In the second part, we propose a new concept of the Field Stop (FS) layer for the diode. Numerical studies demonstrate improved reverse recovery behavior by this type of diode.

## ASYMMETRIC 13-kV THYRISTOR

**Design and preparation details.** The electrically-triggered thyristor investigated consists of a conventional two-stage amplifying gate structure, concentrically surrounding the central gate contact.

The second amplifying gate is distributed in order to trigger the main cathode area as efficiently as possible, so that current spreading is optimized and a sufficient  $dI/dt$  capability is achieved.

The vertical doping profile of the main cathode area is shown schematically in Fig. 1, where  $d_{thy}$  denotes the anode-to-cathode distance of the thyristor,  $d$  the space coordinate along this direction and  $N_D$  the doping concentration of the  $n^-$  base. Float-zone 4-inch silicon wafers with a high resistivity ( $\rho > 500 \Omega\text{cm}$ ) were used as the base material. The deep  $p$  layers were created by two subsequent aluminum vacuum pre-depositions, each followed by a drive-in step. A boron implantation with a subsequent drive-in step was used to improve the contact resistance of the  $p$ -base shorts (not shown in Fig. 1) in the main cathode area of the thyristor. The conventional FS layer and the  $n^+$  emitter were fabricated by two different POCL<sub>3</sub> diffusions. The  $p^+$  emitter—implemented by a standard boron implantation with a subsequent drive-in step—is interrupted by anode shorts (not shown in Fig. 1), which were also created by a masked POCL<sub>3</sub> diffusion. The completely processed wafers typically show charge-carrier lifetimes exceeding 1000  $\mu\text{s}$ .

**Measurement results.** Typical current-voltage characteristics  $I(V)$  in the forward blocking mode are shown in Fig. 2. The asymmetric thyristor is able to block voltages greater than 13 kV at room temperature (25 °C) and elevated temperatures up to 90 °C.

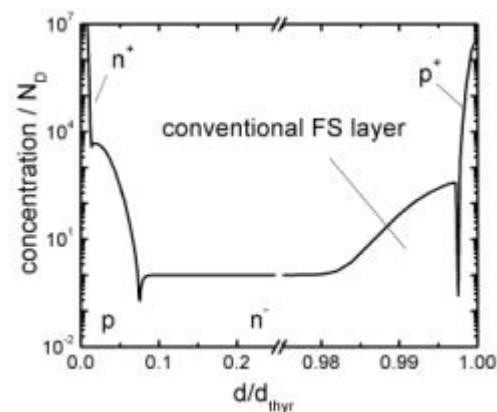


**Figure 1. Schematic vertical doping profile of the thyristor with conventional FS layer**

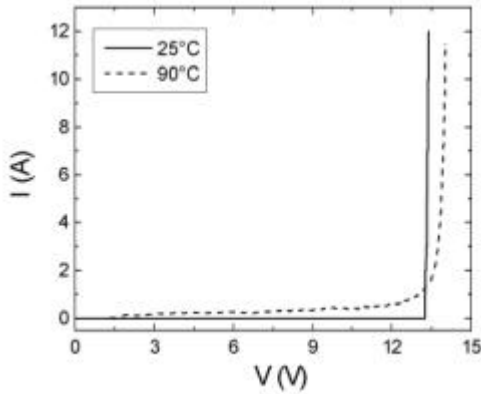


**Figure 2. Forward blocking  $I(V)$  characteristics of the asymmetric 13-kV thyristor**

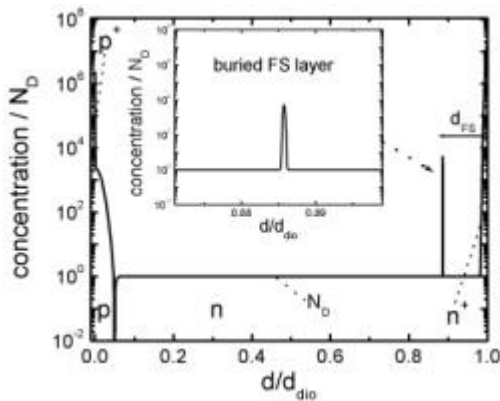


**Figure 3. Schematic vertical doping profile of the diode with buried FS**

The latter is the typical operating temperature in applications such as High-Voltage Direct Current (HVDC) transmission lines. We also prepared diode test structures based on the same base material and subjected to the same process technology except for the cathode and anode emitters. Such diodes are able to withstand reverse voltages exceeding 15 kV.

When all back-end processes are completed, the typical values of the circuit commutated turn-off time are greater than 1000  $\mu\text{s}$ . The on-state voltage is approximately 2.0 V at 4 kA ( $T = 90^\circ\text{C}$ ). Depending on the requirements of the application, these values can be adjusted with an additional electron radiation.

### 13-kV DIODE

**Buried FS layer.** The diode test structures provided with the standard FS layer showed a hard turn-off characteristic under operating conditions typical of HVDC applications. Therefore, we studied a new FS concept based on a relatively small  $n$  layer buried in the  $n^-$  region near the  $n^+$  contact layer (Fig. 3).

To illustrate the effectiveness of the buried FS layer, we compare the turn-off behavior of diodes without and with a buried FS layer. Both diodes have a relatively thick  $n^+$  cathode layer. This layer operates also as an efficient FS layer when the buried FS layer

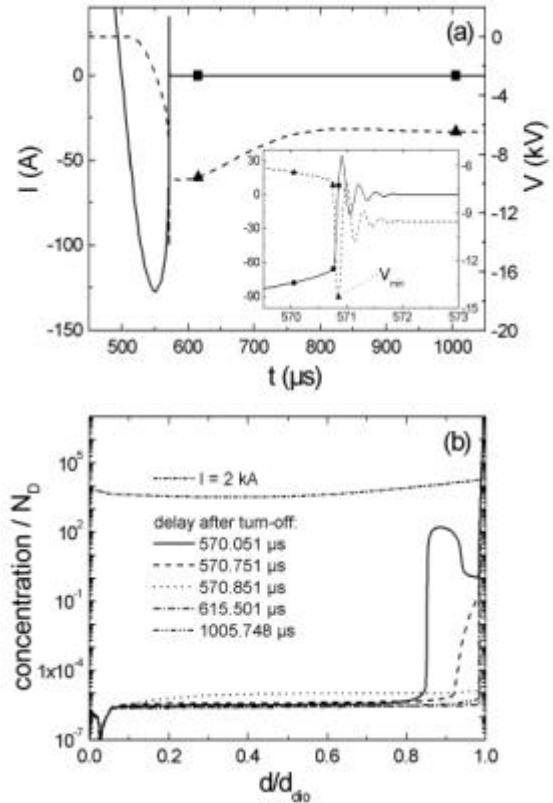


**Figure 4. Turn-off behavior of the diode without buried FS: current and voltage traces (a), electron distributions (b);  $I_{on} = 2$  kA**

is absent or its doping dose, i.e. the doping concentration integrated along this FS layer, is smaller than the so-called breakthrough charge  $Q_C \approx 1.5 \times 10^{12} \text{cm}^{-2}$ . For both diodes, the carrier lifetime in the  $n^-$  region was reduced uniformly as well as locally (close to the anode-side  $p-n$  junction) in such a way that the on-state voltage was about 3.1 V at 4 kA for a contact area corresponding to a 4-inch device.

The turn-off behavior for typical conditions in HVDC applications was analyzed with an  $RCL_S$  element connected in parallel to the diode, where  $L_S$  accounts for unavoidable stray inductance.

The simulations were performed with the device simulator MEDICI [4]. For all simulation results presented below, the load current  $I_{on}$  of the diode was turned off with a current rate of  $-4 \text{ A}/\mu\text{s}$  via an inductance  $L = 1.62 \text{ mH}$ . The operating temperature was  $90^\circ\text{C}$  and a DC link voltage of  $-6.5 \text{ kV}$  was applied during turn-off. The other circuit parameters were  $R = 40 \Omega$ ,  $C = 2 \mu\text{F}$ , and  $L_S = 5 \mu\text{H}$ .

**Diode without buried FS layer.** The reverse recovery behavior of the diode without buried FS is shown in Fig. 4. The transient of the diode current is characterized by a reverse current maximum of about 130 A, followed by a steep current decrease (Fig. 4a). The inset in Fig. 4a shows that both diode current  $I$  and diode voltage  $V$  oscillate for a short period with relatively large amplitude. In Fig. 4b, the electron distribution is depicted at particular times marked in Fig. 4a. The carrier distribution at 2 kA is also

plotted. The steep current drop starting at  $t \approx 570.8 \mu\text{s}$  is strongly correlated to the carrier distribution. At this time, the remaining excess electrons close to the cathode layer vanish, and the current is abruptly interrupted, as no free charge carriers are available to enable a soft reverse recovery. In response to the abrupt current decrease, the electrical circuit—in particular the stray inductance—causes undesired voltage oscillations. It is important to note that the diode shows a similar reverse recovery behavior when it is provided with an additional conventional FS layer, such as the one applied to the thyristor (Fig. 1).

**Diode with buried FS layer.** The turn-off behavior of a diode with a buried FS layer of a doping dose  $Q < Q_c$  is illustrated in Fig. 5. The distance between the narrow FS layer and the cathode emitter is  $\approx 0.13d_{dio}$ , where  $d_{dio}$  denotes the total thickness of the diode. Compared to the diode without buried FS, the reverse recovery behavior is clearly softer. The maximum rate of current decrease during turn-off is distinctly diminished, and although the current and voltage oscillations do not vanish completely, their amplitudes are significantly reduced (Fig. 5a). The electron distributions during turn-off (Fig. 5b) show that the buried FS layer provides additional electrons when the border of the space charge region reaches the FS layer. These additional charge carriers support the continuous current flow in the low-current interval of the recovery period.

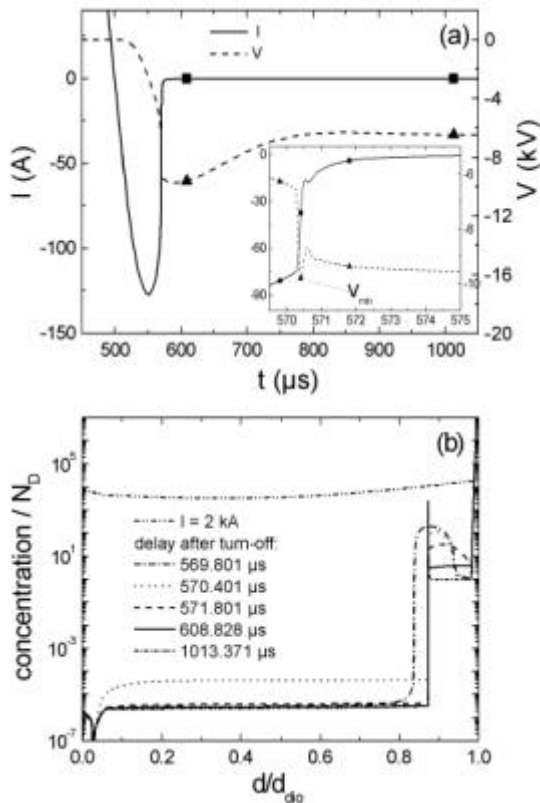


Figure 5. Turn-off behavior of the diode with buried FS: current and voltage traces (a), electron distributions (b);  $I_{on} = 2 \text{ kA}$

The effectiveness of the buried FS layer depends essentially on its distance  $d_{FS}$  from the cathode contact and the doping dose  $Q$ . In Fig. 6, the current traces  $I(t)$  are depicted for different distances  $d_{FS}$ . The reverse recovery behavior becomes softer as  $d_{FS}$  increases. However, for an optimum design we have to consider that the breakdown voltage decreases as  $d_{FS}$  increases.

As a simple measure of softness, we use the minimum value  $V_{min}$  of the voltage trace appearing during turn-off (Figs. 4a and 5a). This value is normalized to the respective breakdown voltage  $V_{br}$  and is plotted in Fig. 7 as function of the distance  $d_{FS}$  for four different doping doses of the buried FS layer. Additionally, the value for the diode without buried FS is drawn as a solid line. The appearance of a minimum in the curves belonging to diodes with a buried FS layer reflects the trade-off relation between the voltage overshoot  $V_{min}$  and the breakdown voltage  $V_{br}$ , both decreasing with increasing  $d_{FS}$ . From this diagram, we estimate that the optimum doping dose  $Q$  of the buried FS layer is  $\approx 4Q_0$  and the optimum distance  $d_{FS}$  is  $\approx 0.13d_{dio}$  for the chosen parameters.

All simulation results considered so far were obtained by turning off the diode from a relative high on-state current of 2 kA, corresponding to a current

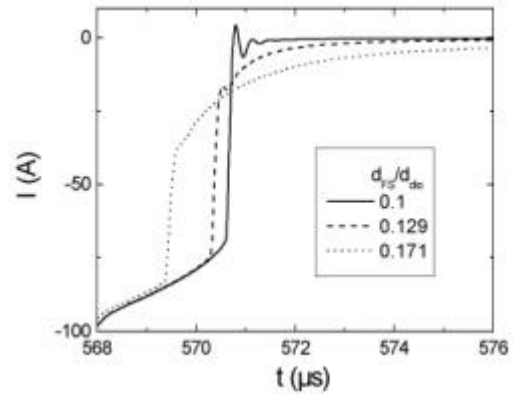


Figure 6. Part of the current traces during turn-off when the excess electrons near the  $n^+$  emitter vanish for different values of  $d_{FS}$

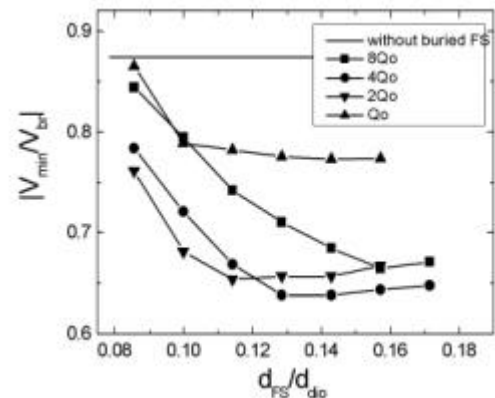


Figure 7. Ratio  $V_{min}/V_{br}$  as function of the ratio  $d_{FS}/d_{dio}$  for different doping doses  $Q$  of the buried FS layer

density  $> 30 \text{ A/cm}^2$ . However, reverse recovery behavior is most critical when the diode is turned off from a relatively low on-state current. In Fig. 5, the voltage and current traces close to the end of reverse current flow are compared for diodes with and without a buried FS layer. Both were turned off from a load current of 100 A, corresponding to a current density  $< 2 \text{ A/cm}^2$ . The doping dose of the buried FS layer and its distance  $d_{FS}$  from the cathode contact were  $4Q_0$  and  $0.13d_{dio}$ , respectively. Obviously, providing the diode with a buried FS layer improves the reverse recovery behavior even at low turn-off currents.

**Fabrication of a buried FS layer.** There are different possibilities to create a buried  $n$ -type FS layer. Because no complex backside patterning is necessary for the diode structures, wafer bonding of a  $p^+n^-$  wafer and an  $n-n^-n^+$  wafer could be a promising technique. In this case, the small  $n$  surface layer of the second wafer acts as buried FS layer after wafer bonding. An alternative method is to use proton implantation followed by an annealing step between 400 and 500 °C for about 30 minutes resulting in hydrogen-related donor formation (e.g. [5,6]). In this temperature range, defect centers such as the divacancy and the vacancy-oxygen defect—which are also generated during proton irradiation and are commonly used to reduce the charge carrier lifetime—anneal out quite efficiently.

We have analyzed the hydrogen-related donor formation in detail by spreading resistance measurements as a function of the irradiation energy, its fluence, and the annealing conditions [7]. The investigations show that creating a buried FS layer for a 13-kV diode is possible with moderate hydrogen fluences.

### SUMMARY

In conclusion, we point out that the fabricated asymmetric thyristor with a conventional FS layer has a forward blocking voltage exceeding 13 kV. For a diode of the same voltage class, numerical studies have shown that the application of a buried FS layer instead of a conventional FS layer results in a softer reverse recovery behavior. This new concept of buried FS layers can also be applied successfully to diodes of lower breakdown voltages. This has been proven by numerical studies for fast 1200-V diodes employed as free-wheeling diodes in a chopper circuit [8]. In any case, the design parameters of the buried FS layer—especially the doping dose and the distance from the cathode contact—need to be adjusted to the particular type of diode and the switching conditions for which the diode is provided. Finally, the results obtained for the 13-kV diode and the thyristor structure suggest that the application of the tandem solution has less power losses than the symmetric thyristor.

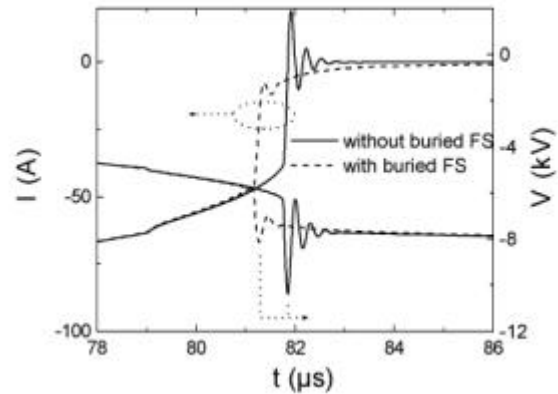


**Figure 8. Reverse recovery behavior for  $I_{on}=100\text{A}$  (buried FS:  $Q=4Q_0$ ;  $d \gg 0.13d_{dio}$ )**

### ACKNOWLEDGMENTS

We would like to thank V. Kartal and M. Ruff for fruitful discussions and R.A. Bommersbach, T. Luse, and C. Schneider for experimental support.

### REFERENCES

- [1] H.P. Lips, J. Matern, R. Neubert, L. Popp, M. Uder, "Light Triggered Thyristor Valve For HVDC Application." *Proceedings of 7<sup>th</sup> European Conference on Power Electronics and Applications, Vol. 1* (1997), pp 1.287.
- [2] J. Przybilla, R. Keller, U. Kellner, C. Schneider, H.J. Schulze, F.J. Niedernostheide, "Applications for direct light triggered thyristors." *Proceedings 2002 International Conference on Power System Technology* (2002).
- [3] J. Przybilla, R. Keller, U. Kellner, C. Schneider, H.J. Schulze, F.J. Niedernostheide, "Direct light triggered thyristors for Pulse-Power-Applications." *Proceedings 2002 European Pulsed Power Symposium* (2002).
- [4] MEDICI, User Manual, Version 2001.4 (2001).
- [5] J. Hartung, J. Weber, "Shallow hydrogen-related donors in silicon." *Phys. Rev. B* 48 (1993), pp 14161.
- [6] H. Iwamoto, H. Haruguchi, Y. Tomomatsu, J.F. Delon, E.R. Motto, "A New Punch-Trough IGBT Having a New n-Buffer Layer." *Proc. IEEE IAS* (1999), pp 692.
- [7] H.-J. Schulze, F.-J. Niedernostheide, M. Schmitt, U. Kellner-Werdehausen, G. Wachutka, "Influence of Irradiation Induced Defects on the Electrical Performance of Power Devices." *ECS-PV: High-Purity Silicon VII* (2003), in press.
- [8] V. Kartal, unpublished results.